Hydraulic modelling of Athabasca Vallis, Mars

DEVON M. BURR*

Departments of Geosciences and Planetary Sciences, University of Arizona, 1629 East University Blvd, Tucson, Arizona 85721, USA

dburr@pirl.lpl.arizona.edu

Abstract Palaeohydraulic modelling is presented for Athabasca Vallis, the youngest known catastrophic flood channel on Mars. This modelling incorporates three significant advantages over previous modelling of Martian channels: a step-backwater hydraulic model; more accurate topography; and improved flood height indicators. The maximum modelled palaeodischarge is between 1×10^6 and 2×10^6 $m^3 s^{-1}$ depending on the friction coefficient selected. An anomalously high palaeostage indicator suggests a region of ponded backwater in the channel in which streamlined forms were created through deposition, with the additional possibility of post-flood subsidence/lowering of the channel slope due to magma extrusion.

Key words Mars; Athabasca Vallis; catastrophic flooding; hydraulic modelling; backwater

Modélisation hydraulique de Athabasca Vallis, Mars

Résumé On présente une modélisation paléo-hydraulique d'Athabasca Vallis, le plus jeune chenal de crue catastrophique connu sur Mars. Cette modélisation présente trois avantages majeurs par rapport aux modélisations précédentes des chenaux de Mars: un modèle hydraulique à casiers; une topographie plus précise; et des indicateurs de niveaux d'eau plus proches de la réalité. La valeur modélisée maximale de paléo-débit se situe entre 1×10^6 et 2×10^6 $m^3 s^{-1}$ selon le coefficient de frottement choisi. Un indicateur de paléo-niveau anormalement haut suggère qu'il y avait des eaux stagnantes dans le chenal au sein duquel des formes d'écoulement se sont créées à travers les dépôts, avec en plus l'éventualité d'une subsidence post-crue et diminution de la pente du chenal, liées à une extrusion magmatique.

Mots clefs Mars; Athabasca Vallis; crue catastrophique; modélisation hydraulique; remous

INTRODUCTION TO ATHABASCA VALLIS

Water plays such a key role in geologic, geophysical, climatic, and potential biotic processes that "follow the water" is the highest priority exploration goal for Mars as stated by the US National Academy of Sciences (2001). Constraining the amount of floodwater previously on the surface of Mars is an important contribution to this strategy. Ares Vallis, one of the largest Martian outflow channels which debouche into Chryse Planitia, measures on the order of 100 km wide, 1300 m deep, and 1500 km long (Komatsu & Baker, 1997; Smith *et al.*, 1998). These circum-Chryse channels have been dated by counting the number and sizes of craters on the channel floors at more than ~2 Ga.

The Athabasca Vallis outflow channel is about an order of magnitude smaller in each dimension than the circum-Chryse channels, but also about three orders of magnitude younger, with a model age of 2–8 Ma (Burr *et al.*, 2002a). Athabasca Vallis is located near Mars' equator at the western edge of the lava-filled Cerberus Plains,

* *Now at:* US Geological Survey Astrogeology Branch, 2255 N. Gemini Drive, Flagstaff, Arizona 86001, USA.

Open for discussion until 1 February 2004

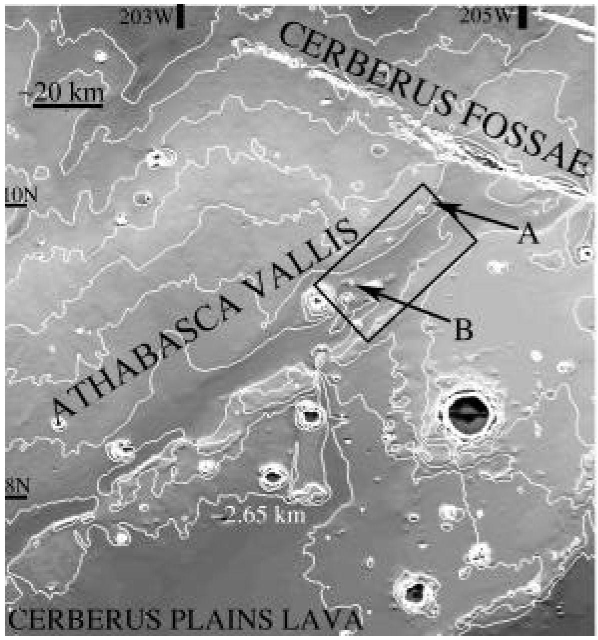

Fig. 1 Topography of the Athabasca Vallis region derived from gridded MOLA data. The black box indicates the modelled reach of Athabasca Vallis. A and B indicate the locations of palaeoflood height indicators shown in Fig. 2A and B. Contour interval is 50 m; white numbers are elevations.

which cover an area greater than 1 million km^2 (Plescia, 1990; Keszthelyi *et al.*, 2000; Sakimoto *et al.*, 2001). The channel system originates at a volcano-tectonic fissure, one of the Cerberus Fossae fissures, as two channels which converge ~25 km downslope into a single main channel (Fig. 1). This main channel is linear due to a linear topographic boundary (a tectonic structure called a "wrinkle ridge") on its southern side. About half way down its length, the channel becomes distributary, with smaller channels cutting through the wrinkle ridge and stretching southward to the Cerberus Plains. The main channel continues to the southwest, where it is buried beneath Cerberus Plains lavas. The entire length of the main channel is ~300 km; its width is 15–30 km, and its depth is 50–100 m (Burr *et al*., 2002b).

Athabasca Vallis is interpreted to be an aqueous flood channel system based on mesoscale geomorphic features that are similar to terrestrial flood-formed features (Tanaka & Scott, 1986; Edgett & Rice, 1995; Burr *et al*., 2002a,b). More than a dozen kilometre-scale streamlined forms are seen in Mars Orbiter Camera (MOC; Malin & Edgett, 2001) images of the main channel, a region that is especially well covered by MOC images as it was a candidate landing site for the Mars Exploration Rovers (McEwen *et al.*, 2002). The streamlined forms are positive relief features, having teardrop or airfoil shapes in plan view. They are similar to streamlined features in the Channeled Scabland of eastern Washington, USA, which were formed by Pleistocene outbursts from glacial Lake Missoula (e.g. Bretz *et al.*, 1956; Bretz, 1969; Baker, 1973). Extensive longitudinal lineations throughout the channel system are similar in size and spacing to longitudinal grooving found in the Channeled Scabland (Burr *et al.*, 2002a,b), which were inferred to have been created by longitudinal vortices in the deep flood flow (Baker, 1978). "Giant current ripples" or subaqueously formed transverse dunes were one of the features most diagnostic of flooding in the Channeled Scabland (Pardee, 1942; Bretz *et al.*, 1956; Baker, 1973). Large dunes transverse to the Athabasca channel have been interpreted to be subaqueously formed dunes as well (Burr *et al.*, 2002a). Glaciers, lava, and CO_2-charged density flows were considered for the formation of this channel, but rejected in favour of catastrophic floodwater flow (Burr *et al.*, 2002a).

IMPORTANCE OF HYDRAULIC CALCULATIONS

An improved estimate of the hydraulic discharge down Athabasca Vallis is important in a number of ways. The floodwater that carved the channel has been hypothesized to have been originally deep groundwater (Burr *et al.*, 2002a), so the catastrophic flood discharge constrains groundwater processes. The water may have emerged from the fissures as a plume several kilometres tall (Burr *et al.*, 2002a), so that calculations would also provide information on the amount of recent water vapour input into the Martian atmosphere. Both the floodwaters (Burr *et al.*, 2002a,b), and the Cerberus Plains lava flows (Plescia, 1990; Keszthelyi *et al.*, 2000; Sakimoto *et al.*, 2001) emerged from the Cerberus Fossae, so that discharge calculations could be an important constraint on local volcano-groundwater/ice interactions.

PALAEOFLOOD ANALYSIS ON EARTH

Palaeoflood analysis involves deducing a past flood's discharge and other flow parameters from topographic and geomorphic evidence (e.g. Patton *et al.*, 1979; Baker *et al.*, 1983; Jarrett & Malde, 1987; O'Connor & Baker, 1992; O'Connor, 1993). The term implies the use of computer hydraulic models into which are input a variety of hypothetical discharges; the discharge whose modelled floodwater height best fits the geological evidence of the palaeofloodwater height is taken to be the best palaeo-discharge estimate (O'Connor & Webb, 1988). Thus, accurate palaeoflood analysis requires (a) a physically representative hydraulic model, (b) an accurate topographic representation of the channel at the time of the flow, and (c) solid geological evidence of the palaeoflood height.

Examples of terrestrial catastrophic palaeoflood discharge analysis include those for the Spokane flood from glacial Lake Missoula that carved the Channeled Scabland (O'Connor & Baker, 1992) and for the Lake Bonneville flood down the Snake River in Idaho, USA (O'Connor, 1993). The modelling in these terrestrial examples was accomplished with the HEC-2 model, developed by the US Army Corps of Engineers Hydrologic Engineering Center. Like other step-backwater models, HEC-2 and its successor HEC-RAS balance potential energy, kinetic energy, and frictional energy loss between cross-sections, stepping up- or downstream as the flow is sub- or supercritical (O'Connor & Webb, 1988; Hydrologic Engineering Center, 2001). The energy loss between cross-sections is partitioned into frictional losses (evaluated with Manning's equation), and transition losses. These HEC models assume that flow is uniform in time and steady or gradually varied in space (O'Connor & Webb, 1988; Hydrologic Engineering Center, 2001).

PALAEOFLOOD MODELLING FOR ATHABASCA VALLIS

Previous peak discharge estimates for older Martian channels, which used a wide spectrum of hydraulic models, topography and assumed water heights, have varied by several orders of magnitude (e.g. Carr, 1979; Baker & O'Connor, 1988; Komatsu & Baker, 1997; Smith *et al.*, 1998). The Athabasca channel palaeoflood estimates presented here benefit from three improvements over previous efforts: a more recent hydraulic model, more accurate topography, and better geological constraints on palaeoflood height.

Computer model: Martian version of HEC-RAS

The hydraulic model HEC-RAS Version 3.0 (Hydrologic Engineering Center, 2001) used in this modelling is a step-backwater model also commonly used in terrestrial palaeohydrology. For this application to Mars, the acceleration of gravity in HEC-RAS was reduced to the Martian value of 3.71 m s^{-2}, the specific weight of water was reduced to 3711 N m^{-3}, and the Manning's *n* value was adjusted for Martian gravity. Calculating Manning's *n* for a given depth of flow, via a dimensionless drag coefficient, is equivalent to multiplying it by the square root of the ratio of terrestrial to Martian gravity (derived from Komar, 1979), which equals 1.62 (e.g. Komatsu & Baker, 1997).

Selection of Manning's *n* value Evidence points to lava as the substrate of Athabasca Vallis. The vast Cerberus Plains just to the south are filled with basaltic lava, at least some of which emanated from the same Cerberus Fossae fissures as the floodwater (Plescia, 1990; Keszthelyi *et al.*, 2000; Sakimoto *et al.*, 2001). Lava is suggested by dark, textured, lobate surfaces adjacent to the Athabasca Vallis channel (Burr *et al.*, 2002b), and by dark, resistant layers in both the Cerberus Fossae walls and in bedrock knobs in the channel (e.g. Fig. 5, Burr *et al.*, 2002a). Recent observations from the Mars Odyssey spacecraft suggest that lava erupted from the same reach of fissure and followed the same overall path as the floodwater (McEwen *et al.*, 2002).

Basalt or other igneous lithologies are not commonly indexed in tables of Manning's *n* values (e.g. Chow, 1964, pp. 7–25; Hydrologic Engineering Center, 2001, pp. 3-13–3-15). The magnitude of the flow also adds uncertainty, as any well-calibrated values of Manning's *n* were deduced for a channel orders of magnitude more shallow than Athabasca Vallis. Creek beds composed of lava or large boulders resulted in Manning's *n* values as high as 0.2 during extremely low flows, but the values rapidly decreased to well under 0.1 with only slight (i.e. a few m^3 s^{-1}) flow increase (Hicks & Mason, 1991). To model the discharge from glacial Lake Missoula, which flowed over Columbia River basalt, O'Connor & Baker (1992) used *n* values of 0.04 for the valley floor, 0.05 for the valley walls, and 0.1 for flow over the uplands. In modelling the Lake Bonneville Flood, which flowed over the basaltic Snake River plains, O'Connor (1993) used 0.03 for the main channel, 0.05 for the valley walls or stripped basalt, and 0.06–0.1 for butte and basin scabland. These values gave good fits to the geologic palaeoflood indicators for most of the modelled reaches.

The Manning's *n* values used in this Athabasca modelling encompassed those in the low to moderate range of values used in these previous terrestrial palaeoflood applications. Specific formations associated with higher Manning's *n* values (such as butte and basin topography in the Channeled Scabland) could not be identified. And, as indicated by calibrated data (Hicks & Mason, 1991), effective Manning's *n* values appear significantly reduced by large or deep flows. Consequently, this study used minimum and maximum Manning's *n* values of 0.03 and 0.06. These terrestrial values were converted to Martian equivalent values by multiplying by 1.62 as explained above, resulting in Martian values of 0.048 and 0.097. This factor of two in the Manning's *n* values results in a factor of two in the discharge.

Selection of expansion and contraction coefficients Given the channel's linear form, this modelling used channel contraction and expansion values for gradual transitions of 0.1 and 0.3, respectively (Hydrologic Engineering Center, 2001, pp. 3–20). Varying the values within reasonable limits produces an insignificant effect on the flow profile. This is likely due to the wide, shallow character of Athabasca Vallis, in which loss due to turbulence is minimal compared to loss due to friction exerted by the channel, and any resultant variation in flow height is spread over a wide channel.

Boundary conditions Given the shallow slope (0.0006 m m^{-1}), lower Martian gravity, and wide, shallow character of Athabasca Vallis, flow was modelled as subcritical. Normal flow was selected as the boundary condition, and subcritical flow was selected as the flow regime. The resultant modelled Froude numbers were generally between 0.3 and 0.5, with a highest Froude number of 0.76 at the upstream end of the reach. The model was also run with critical boundary conditions and a mixed flow regime, which produced almost identical, subcritical, Froude numbers.

Topographic input

The HEC-RAS model requires river cross-sections. For Athabasca Vallis, these cross sections were taken from a digital elevation model of Mars Orbiter Laser Altimeter (MOLA) data (Zuber *et al.*, 1992; Smith *et al.,* 1998). MOLA takes a topographic measurement every ~300 m along track. Because the spacecraft is in a polar orbit, the spacing between tracks at the equator is often several kilometres wide, and only about a dozen individual tracks cross the Athabasca study reach. As this spacing is too low for HEC-RAS computational closure, cross-sections were derived from interpolated MOLA data. Natural neighbour interpolation has been shown to create the most realistic topography (Abramov & McEwen, 2002), and was used in this study. This DEM was imported into the Interactive Data Language (IDL) program "gridview," created by MOLA team members (Roark & Frey, 2001), which allows derivation of linear topographic profiles. Thirty-one profiles were taken perpendicular to the ~60 km reach, and input as cross-sections into HEC-RAS.

High-water marks

The reach of Athabasca Vallis below the confluence was chosen for the hydraulic modelling (Fig. 1). This upper reach is linear with no apparent tributary or distributary channels and has better constraints on the water profile than the more distal, or lower, part of the channel. To ensure that the geologic evidence defines a distinct palaeoflood profile, the length of a modelled reach should be “several times” greater than its width (O’Connor & Webb, 1988, p. 399), so the length of the Athabasca Vallis modelled reach is slightly short in relation to its large width; however, a modelled reach of any greater length would extend into the distributary part of the channel.

HEC-RAS assumes gradually varied flow so that the entire reach is affected simultaneously by the peak discharge. This requirement is hard to verify for Athabasca Vallis, because neither the input hydrograph nor the likelihood of kinematic waves can be deduced. In channel reaches a significant distance from the source outlet, kinematic waves would be damped out. The modelled reach of Athabasca Vallis is ~20 km from the source, and it is possible that the high water marks were emplaced during the passage of a kinematic wave. If so, this would probably cause the modelled discharge to be higher than the actual discharge.

Palaeostage indicators in conjunction with MOLA elevations provide constraints for modelling. Thus, to be useful in this study, an indicator had to be identifiable in a MOC image for which there is an associated MOLA track (two examples are shown in Fig. 2). Although the channel received good MOC coverage during its former status as a potential landing site (McEwen *et al.*, 2002), MOLA had by that time ceased returning data. So MOLA tracks for the geomorphic palaeoflood indicators in MOC images are few. In this ~60-km long study reach, a total of six (maximum and minimum) palaeostage constraints were found (Fig. 3).

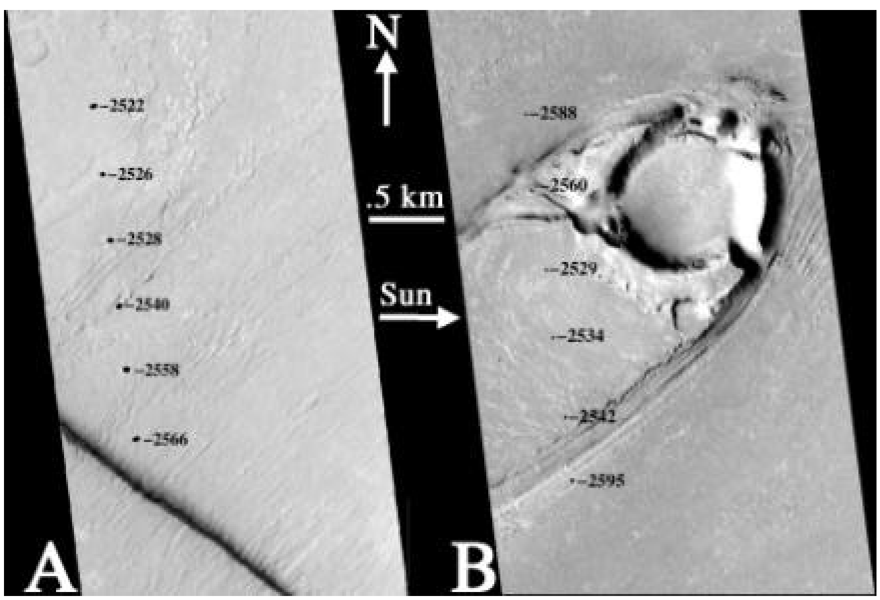

Fig. 2 Two palaeoflood height indicators used as hydraulic modelling constrains. These figures are portions of MOC images overlain with individual MOLA elevations. A: Portion of MOC image M02-01973, showing longitudinal lineations in the channel interpreted as created by catastrophic flood flow, whereas the unlineated terrain north of the channel is interpreted as not having been flooded. Maximum palaeoflood height is interpreted as being approximately –2528 m, minimum as approximately –2560 m. B: Portion of MOC image M07-00614, showing a streamlined form interpreted as having formed primarily by deposition of sediment from the ponded floodwaters. Minimum palaeoflood height is interpreted as being –2529 m. Figure A is ~35 km upslope of Figure B.

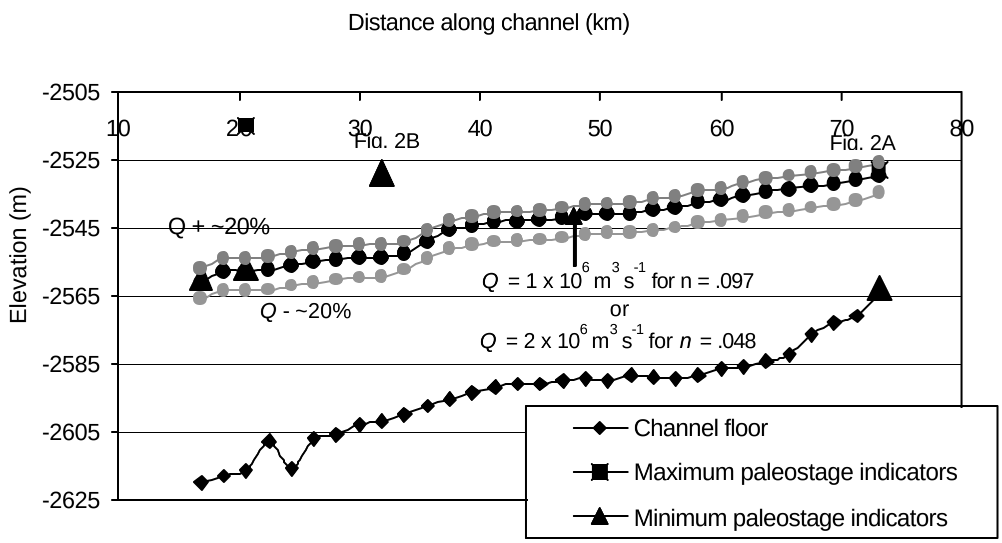

Fig. 3 Plot of channel topography and modelled water height. The modelled profile is both for $Q = 1 \times 10^6$ m^3 s^{-1} for $n = 0.097$, and $Q = 2 \times 10^6$ m^3 s^{-1} for $n = 0.048$; ~20% higher and lower discharge profiles are also plotted, and palaeoflood height indicators in Fig. 2 are labelled. The minimum palaeoflood height indicator labelled "Fig. 2B" exceeds the modelled palaeoflood height, and is hypothesized to have been formed by sediment deposition during floodwater ponding behind the large crater at the downstream end of the modelled reach.

Channel margins Some geomorphic constraints on the floodwater height come from the channel margins, which show distinct cut-offs between the topographically higher bank and the longitudinally lineated (i.e., diluvially eroded) channel (Fig. 2A). The heights on the MOLA track of these erosional boundaries are used as high water marks.

Streamlined mesas Other palaeostage indicators are "streamlined mesas," flat-topped, layered, streamlined forms hypothesized to be formed primarily by subaqueous deposition of sediment in the lee of a resistant obstacle, such as a bedrock knob or an impact crater (Burr *et al.,* 2002b). According to this mode of formation, the downslope portions of these streamlined mesas would mark the minimum peak water heights during their formation (Fig. 2B). Analogous depositional constraints (i.e. eddy and slackwater deposits) were used by O'Connor & Baker (1992) as minimum peak water heights for the Lake Missoula flood.

MODELLING RESULTS

An indication of ponding

The accuracy of hydraulic modelling is reflected in the fit of the modelled water surface to the geologic palaeoflood evidence (O'Connor & Webb, 1988). Of the six palaeostage indicators along this reach, the modelled discharges fit five of them (Fig. 3). That is, the modelled water surface is at or below the two maximum palaeostage indicators, and at or above three of the four minimum palaeostage indicators. The fourth minimum palaeostage indicator (Fig. 2B), which should be at or below the modelled water surface, is instead above it. Its minimum elevation of –2529 m is approximately equal to the maximum elevation of –2528 m of the most upslope palaeostage indicator (Fig. 2A), located ~35 km upslope (see elevations on Figs 2 and 3). Given the average channel slope of 0.0006, these two indicators should have been ~20 m different in elevation.

This lack of difference in elevation is hypothesized here to be due to temporary ponding of the floodwater upstream of the large impact crater in the channel (at the lower end of the modelled reach, as seen in Fig. 1). The impact crater and its now-eroded ejecta blanket would have constricted or blocked the channel, possibly enough to temporarily pond the floodwater. When the water overtopped or broke through the ejecta dam, it would have washed away much of the ejecta blocking the channel. The effect from the crater on the channel width is still apparent, however, as the channel, which is 15–20 km wide for most of its length, expands to 30 km wide around the crater. This hypothesized ponding provides an explanation for the strong clustering of streamlined mesas in the modelled reach, as a result of deposition in the slower or stagnant flow. The subsequent break-through of the ejecta dam and outrush of the ponded water would have carried away most of the deposits except for those protected behind impact craters or other obstacles.

Additionally, the lack of elevation difference could be due to post-eruption subsidence. Since both lava and water erupted from the same fissure (Burr *et al.*, 2002b; McEwen *et al.*, 2002), it is possible that the channel was steeper during flood flow but decreased to its current shallow slope due to post-flood, post-magma extrusion subsidence. If this were the case, using the current slope in modelling would underestimate the flow velocity and discharge. However, the preponderance of streamlined forms upstream of the impact crater in the channel would still require explanation, which is provided with the hypothesis of ponding. Post-magma extrusion subsidence could be an additional factor, but not the sole cause, of the lack of elevation difference.

If the streamlined form were bedrock, instead of the hypothesized sediment, it would still provide a high water mark. The layered upper surface is smoother and less cratered than the terrain surrounding the channel, so its upper surface was likely eroded by palaeoflood water reaching the top of the form. However, if this and the other streamlined forms are eroded bedrock, their clustering in this location would be difficult to explain; velocity flow would have been reduced due to channel constriction and friction around the impact crater, and bedrock erosion thereby minimized. A sedimentary composition can easily explain the forms' clustering upstream of the crater as a natural consequence of ponding. Both their morphology and their location support the hypothesis that these flat-topped streamlined forms are depositional.

Hydraulic parameters

Maximum instantaneous discharge For the Manning's *n* value of 0.048, the instantaneous volumetric discharge whose water profile most closely correlated with the geomorphic evidence was 2×10^6 $m^3 s^{-1}$. For the Manning's *n* value of 0.097, the most closely correlated discharge was 1×10^6 $m^3 s^{-1}$ (Fig. 3). These HEC-RAS model values are for clear water flow, whereas the flood would have been a mixture of water and significant amounts of sediment (Komar, 1980). This sediment would have taken up some of the volume implicitly attributed to water, so that the discharge of water alone would have been less than the modelled discharge. The modelling also implicitly assumes the channel topography and geomorphology to have been created by a single flood. However, there was probably more than one flood (Burr *et al.*, 2002a), which may have incised the channel during or subsequent to the formation of the geomorphic features. This lowering of the channel floor relative to the geomorphic palaeoflood height indicators would create an artificially large modelled cross-sectional area compared to the actual cross-sectional area at the time of flooding. So for both these reasons, these modelled discharge values are probably maximum values for the instantaneous flow of water alone down the channel. Conversely, the current topography could be shallower than the flood topography due to lava or other infill. Ongoing work is investing this possibility.

RELEVANCE TO FUTURE MARS EXPLORATION

The modelling results presented here demonstrate the value of recently acquired, higher resolution data of Mars (available at http://pds.jpl.nasa.gov). Such results are the foundation of the continued international Mars exploration programs of the US National Aeronautics and Space Administration (NASA) and the European Space Agency (ESA). Specifically, they bolster the case for interpretation of streamlined forms as composed of flood-deposited sediment, possibly from within the Cerberus Fossae, which may make them attractive targets for future landed exploration.

Acknowledgements Steve Piper provided me with a version of HEC-RAS's steady flow module with Martian parameters, and Prof. Kevin Lansey provided repeated discussions about this application of HEC-RAS. I also thank Profs Victor Baker, Paul Carling, Alfred McEwen, and Dr Hideaki Miyamoto for helpful discussions, and Dr Jim O'Connor for a very helpful review. I acknowledge support from NASA's GSRP at Goddard Space Flight Center (award NGT5-110).

REFERENCES

Abramov, O. & McEwen, A. S. (2002) An evaluation of interpolation methods for Mars Orbiter Laser Altimeter (MOLA) data, *EOS Trans. Am. Geophys. Union* **82**(47), *Fall Meet. Suppl.* (abstract P42A-0567).

Baker, V. R. (1973) Paleohydrology and sedimentology of Lake Missoula flooding in eastern Washington. *Geol. Soc. Am. Spec. Paper* **144**.

Baker, V. R. (1978) Large-scale erosional and depositional features of the Channeled Scabland. In: *The Channeled Scabland* (ed. by V. R. Baker & D. Nummedal) (Proc. Comparative Planetary Geology Field Conf., Columbia Basin), 81–115. NASA, Washington, DC, USA.

Baker, V. R., Kochel, R. C., Patton, P. C. & Pickup, G. (1983) Paleohydrologic analysis of Holocene flood slack-water sediments. *Spec. Publ. Int. Assoc. Sedimentol.* **6**, 229–239.

Baker, V. R. & O'Connor, J. E. (1988) Peak flows for cataclysmic floods. National Aeronautics and Space Administration Tech. Memo. 4041, 299–301.

Bretz, J. H. (1969) The Lake Missoula floods and the Channeled Scabland. *J. Geol.* **77**, 505–543.

Bretz, J. H., Smith, H. T. U. & Neff, G. E. (1956) Channeled Scabland of Washington: new data and interpretations. *Geol. Soc. Am. Bull.* **67**, 957–1049.

Burr, D. M., Grier, J. A., McEwen, A. S. & Keszthelyi, L. P. (2002a) Repeated aqueous flooding from the Cerberus Fossae: evidence for very recently extant, deep groundwater on Mars. *Icarus* **159**(1), 53–73.

Burr, D. M., McEwen, A. S. & Sakimoto, S. E. H. (2002b) Recent aqueous floods from the Cerberus Fossae, Mars. *Geophys. Res. Lett.* **29**(1), 10.1029/2001GL013345.

Carr, M. H. (1979) Formation of Martian flood features by release of water from confined aquifers. *J. Geophys. Res.* **84**(B6), 2995–3007.

Chow, V. T. (ed.) (1964) *Handbook of Applied Hydrology: a compendium of water-resources technology.* McGraw-Hill, New York, USA.

Edgett, K. S. & Rice, J. (1995) Very young volcanic, laucustrine, and fluvial features of the Cerberus and Elysium basin region, Mars: where to send the 1999 Mars surveyor lander. *Lunar Planet. Sci.* **XXVI**, 357–358 (abstract).

Hicks, D. M. & Mason, P. D. (1991) Roughness characteristi cs of New Zealand rivers. *Water Resources Survey*. DSIR Marine and Freshwater, New Zealand.

Hydrologic Engineering Center (2001) *HEC-RAS Hydraulic Reference Manual, version 3.0*. CPD-69, US Army Corps of Engineers Hydrologic Engineering Center, Davis, California, USA.

Jarrett, R. D. & Malde, H. E. (1987) Paleodischarge of the late Pleistocene Bonneville Flood, Snake River, Idaho, computed from new evidence. *Geol. Soc. Am. Bull.* **99**, 127–134.

Keszthelyi, L. P., McEwen, A. S. & Thordarson, Th. (2000) Terrestri al analogs and thermal models for Martian flood lavas. *J. Geophys. Res.* **105**(E6), 15,027–15,049.

Komar, P. D. (1979) Comparisons of the hydraulics of water flows in Martian outflow channels with flows of similar scale on Earth. *Icarus* **37,** 156–181.

Komar, P. D. (1980) Modes of sediment transport in channelized water flows with ramifications to the erosion of the Martian outflow channels. *Icarus* **42**, 317–329.

Komatsu, G. & Baker, V. R. (1997) Paleohydrology and flood geomorphology of Ares Vallis. *J. Geophys. Res.* **102**(E2), 4151–4160.

Malin, M. C. & Edgett, K. S. (2001) Mars Global Surveyor Mars Orbiter Camera: interplanetary cruise through primary mission. *J. Geophys. Res.* **106**(E10), 23,429–23,570.

McEwen, A. S., Keszthelyi, L. P., Milazzo, M., Burr, D. M. Christensen, P. R., Rice, J., Malin, M. & THEMIS team (2002) Athabasca Valles Region: new insights from THEMIS. *EOS Trans. Am. Geophys. Union* **83**(47) *Fall Meet. Suppl*. (abstract P11B-09).

O'Connor, J. E. (1993) Hydrology, hydraulics, and geomorphology of the Bonn eville flood. *Geol. Soc. Am. Spec. Paper* **274**.

O'Connor, J. E. & Baker, V. R. (1992) Magnitudes and implications of peak discharges from glacial Lake Missoula. *Geol. Soc. Am. Bull.* **104**, 267–279.

O'Connor, J. E. & Webb, R. H. (1988) Hydraulic modeling for paleoflood analysis. In: *Flood Geomorphology* (ed. by V. R. Baker, R. C. Kochel & P. C. Patton), 393–402. John Wiley & Sons Inc., New York, USA.

Pardee, J. T. (1942) Unusual currents in glacial Lake Missoula, Montana. *Geol. Soc. Am. Bull.* **53**, 1569–1600.

Patton, P. C., Baker, V. R. & Kochel, R. C. (1979) Slackwater deposits: a geomorphic technique for the interpretation of fluvial paleohydrology. In: *Adjustments of the Fluvial System* (ed. by D. D. Rhodes & G. P. Williams), 225–253. Kendall/Hunt Publ. Co., Dubuque, Iowa, USA.

Plescia, J. B. (1990) Recent flood lavas in the Elysium region of Mars. *Icarus* **88**, 465–490.

Roark, J. H. & Frey, H. V. (2001) GRIDVIEW: recent improvements in research and education software for exploring Mars topography. *Lunar Planet. Sci.* **XXXIII** (abstract 1618).

Sakimoto, S. E. H., Riedel, S. J. & Burr, D. M. (2001) Geologically recent Martian volcanism and flooding in Elysium Planitia and Cerberus Rupes: plains-style eruptions and related water release? *Geol. Soc. Am. Annual Meeting* (abstract 25341).

Smith, D. E., Zuber, M. T., Frey, H. V., Garvin, J. B., Head, J. W., Muhleman, D. O., Pettengill, G., H., Phillips, R. J., Solomon, S. C., Zwally, H. J., Banerdt, W. B. & Duxbury, T. C. (1998) Topography of the northern hemisphere of Mars from the Mars Orbiter Laser Altimeter. *Science* **279**, 1686–1692.

Tanaka, K. L. & Scott, D. H. (1986) The youngest channel system on Mars. *Lunar Planet. Sci.* **XVII**, 865–866 (abstract).

US National Academy of Sciences (2001) Space Studies Board, COMPLEX report. http://www.nationalacadmeis.org/ssb/bibl.html.

Zuber, M. T., Smith, D. E., Solomon, S. C., Muhleman, D. O., Head, J. W., Garvin, J. B., Abshire, J., B. & Bufton, J. L. (1992) The Mars Observer Laser Altimeter investigation. *J. Geophys. Res.* **97**, 7781–7797.

Received 11 November 2002; accepted 21 April 2003